High-density femtosecond transient absorption spectroscopy of semiconductor nanoparticles. A tool to investigate surface quality*

C. Burda and M. A. El-Sayed*

Laser Dynamics Laboratory, School of Chemistry and Biochemistry, Georgia Institute of Technology, Atlanta, Georgia 30332-0400 USA

Abstract: At the high laser excitation intensities used in our experiments, more than 50 electron-hole pairs are formed in colloidal semiconductor nanoparticles used in our studies. At this density of charge carriers, new transient absorptions are observed in the femtosecond transient spectra in the 450 to 700 nm region with unresolved fast rise (<100 fs) and two decay components of 660 fs and >150 ps. The absorption at 510 nm could be quenched with the adsorption of electron acceptors (e.g., benzoquinone, 1,2-naphthoquinone), whereas the low-energy transient absorption was not affected. For CdS NPs, we found that passivation eliminated most of the transient absorption. The transient absorptions are thus proposed to result from either trap-state absorption, trapped dimers (or complexes) and/or Stark-shifted exciton absorption resulting from surface electric field of the uncompensated trapped electron-hole pairs. All these possibilities require effective surface trapping at these high levels of excitation.

INTRODUCTION

With the application of femtosecond spectroscopy to semiconductor nanoparticles it became possible to follow the dynamics of the optical excitations directly in "real-time". The characteristic time constants of the elementary relaxation times can be as short as a few tens of femtoseconds. The material accumulated in this rapidly growing field is huge and can be followed from the Proceedings of the International Conference Series on the Physics of Semiconductors, on Ultrafast Phenomena, Nonlinear Optics and Excitation Kinetics in Semiconductors (NOEKS), and the IUPAC Workshop on Advanced Materials (WAM).

In the following, an introduction to the elementary relaxation processes occuring in semiconductor nanoparticles is given. This will be followed by results and discussion of the origin of the new high-density absorptions observed in femtosecond transient spectra. The basic relaxation mechanisms in semiconductors, which follow the short electronic excitation, can be discussed in the limits of weak coupling. However, for small particles under intense excitations, this idealized picture is complicated. In addition, surface effects lead to fast trapping processes. In fact, surface trapping is among the fastest relaxation events in photoexcited semiconductor nanoparticles and can occur on the femtosecond- and picosecond time scale. To study the effect of surface traps on the spectral dynamics, samples with different surfaces were prepared and investigated by pump-probe spectroscopy. The consequences of surface trapping under high-density excitation condition are discussed in this paper.

Elementary relaxation processes in semiconductor nanoparticles

With a femtosecond laser pulse an electronic excitation is created. The polarization of the excited nanoparticle (NP) is initially in phase (i.e., coherent) with the incident electromagnetic field. The first scattering events will destroy this initial coherence [1]. The lifetime of the coherent polarization is called pure phase-relaxation time (T_2). Possible origins for scattering are lattice defects, impurities, phonons (so-called Froehlich interaction, deformation potential and piezo-coupling), excited electrons, or other excitons [1,2].

The next step during the lifetime of an electron-hole pair is the intraband relaxation, sometimes designated by T_3. Intraband relaxation for excess energies above the bottom of the band usually takes place by emission of optical phonons [3]. This process takes place on the femtosecond or picosecond time domain and was studied in detail for CdSe NPs [2]. The rest of the energy has to be dissipated [4] by emission of smaller energy quanta-like acoustic phonons. This process becomes progressively slower with decreasing energy, which leads potentially to a "phonon bottleneck" [3]. If the lifetime of an intrinsic electronic excitation (excitons) is long enough, it thermalizes with the lattice, reaches Boltzmann distribution, and can be described in thermodynamic terms, e.g., with a temperature.

Even without any scattering process, the phase will ultimately be lost in the charge-carrier recombination process. This recombination lifetime is labeled as T_1 and it necessarily holds $T_2 \leq T_1$ and $T_2 \leq T_3$. But T_1 and T_3 are not correlated. It should be mentioned that both T_1 and T_3 contribute to the dephasing of the system. The recombination process can occur radiatively or nonradiatively. For a direct band gap semiconductor, T_1 is on the nanosecond time scale and emission quantum yields between 10^{-3} and ≤ 1 are observed [5]. For an indirect gap material, T_1 is in the μs to ms range and the emission quantum yields can be extremely low because of the small radiative probability as dictated by the selection rules. Besides the uni-molecular electron-hole recombination process described by T_1, there are higher-order recombination processes like nonradiative Auger recombination, which is a three-particle process, [1] where the energy is absorbed by another electron or hole. These processes are of importance in high-density electron-hole pair systems. The effect of the high exciton density on the transient absorption was studied on CdSe NPs [6]. Figure 1 summarizes some of the elementary relaxation mechanisms for semiconductor NPs in an energy diagram.
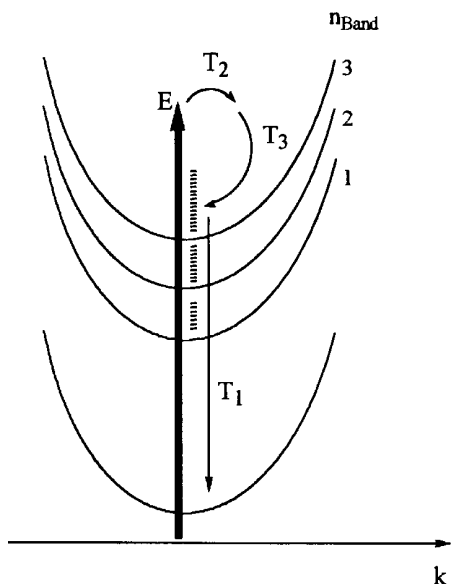

Fig. 1 The energy diagram of bulk semiconductor showing the different possible elementary relaxation mechanisms of a photoexcited semiconductor leading to charge recombination (with lifetime T_1), phase-relaxation ($T_2 < T_1$), and intraband relaxation (T_3).

Effect of the nanoparticle surface on the exciton relaxation

In addition to the processes observed in the bulk, surface trapping offers a very probable relaxation process for the electron and holes in semiconductor nanoparticles. One reason why semiconductor NPs are promising for materials applications is their large surface-to-volume ratio, which enhances charge carrier interactions at interfaces. This is especially true when the nanoparticle radius is smaller than the exciton Bohr radius and, as a result, the wave function of one of the charge carriers has a large amplitude near the interface. These interfacial processes are important for applications in photocatalysis and in devices such as nanocrystaline diodes [7] or solar cells [8]. It is important to understand the charge-carrier confinement and surface trapping phenomena as semiconductor technology moves from the micro- to the nanoscale. A trap state can generally be characterized as a state with decreased overlap of the electron and hole wave functions. The extent of the overlap reduction depends greatly on the spatial extension and energetic depth of the trapping sites. Unfortunately, the trapping sites, which are responsible for the carrier capture, are not observable with direct spectroscopic means and might only be assigned to the long-wavelength tail of the absorption spectra. Somewhat easier is the detection of surface traps by emission spectroscopy, but their analysis certainly needs careful time- and temperature-dependent investigations. On the other hand, band-edge luminescence and a shallow trap emission are very difficult to distinguish.

As we will point out below, high-density femtosecond spectroscopy is an interesting alternative to detect the trapping sites of a nanoparticle. Femtosecond transient absorption spectra of semiconductor nanoparticles show strong nonlinear pump power dependence. In addition, the energetic positions and band shapes of the transient spectra depend on the surface conditions. Several studies of the laser-induced transient absorption of semiconductor NPs have been reported [9–21]. The transient absorption might have contributions from the band edge carriers, trapped carriers, and solvated carriers. The discussion in this paper attempts to clarify which mechanism is responsible for the power-dependent transient absorption of the investigated nanoparticles.

EXPERIMENTAL

The 4-nm-diameter CdSe NP samples were prepared according to the procedure developed by Murray, et al. [22], the CdS NPs following the procedure by Spanhel et al. [23].

Our femtosecond transient absorption experiments were carried out with an amplified Ti-Sapphire laser system (Clark MXR CPA 1000). It was pumped by a diode-pumped, frequency-doubled Nd:Vanadate laser (Coherent Verdi). This produced laser pulses of 100 fs duration (HWFM) and an energy of 1 mJ at 790 nm. The repetition rate was 1 kHz. A small part (4%) of the fundamental was used to focus in a 2-mm sapphire plate to generate a white light continuum which was used between 430–780 nm. The excitation beam was modulated by an optical chopper (HMS 221) with a frequency of 500 Hz. The probe light was split into a reference and a signal beam. The samples were irradiated in cylindrical cuvettes of 2-mm optical path length, placed in a spinning sample holder. After passing the monochromator (Acton Research) both beams were detected by two photodiodes (Thorlab). The kinetic traces were obtained using a sample-and-hold unit and a lock-in-amplifier (Stanford Research Systems). The typical measured optical density (OD) changes were in the range of 50 mOD. For spectral measurements a CCD camera (Princeton Instruments) attached to a spectrograph (Acton Research) was used. The group velocity dispersion of the white light continuum was compensated. The absolute laser power was adjusted by an appropriate aperture, the relative power with a filter wheel.

Femtosecond pump-probe spectra of the colloidal CdSe NPs with 4 nm diameter in toluene were recorded as a function of pump intensity. The excitation wavelength was 400 nm, and all other experimental conditions were kept constant during the course of the measurements. The samples were mea-

sured as colloidal solutions at room temperature in fast-rotating quartz cells. No optical degradation was observed after each experiment, which we check by UV–vis absorption, fluorescence spectroscopy, and TEM measurements.

RESULTS

Nanoparticles with low density of surface traps: CdSe NPs

The laser power dependence of the femtosecond transient absorption spectra is measured for a series of experiments, where the pump power was increased in steps of 4 mJ/cm^2. Figure 2 shows the transient absorption spectra of the CdSe NPs, pumped with 400 nm fs-laser pulses. The presented transient absorption features are the spectral changes observed by step-wise increasing the pump power. At the lowest possible laser power the bleach spectra of the two exciton transitions at 560 and 480 nm are resolved. According to the state filling model [24,25] the lowest energy bleach band at 560 was assigned to the $|1s_e, 1s_h>$ state and the second bleach band at 480 nm to the strong transition to the $|1p_e, 1p_h>$ state. If the pump pulse was adjusted to an intermediate laser flux (6 to 12 mJ/cm^2), while the beam characteristics and the solution remained unchanged, the transient spectra still show the bleach of the $1s_e$–$1s_h$ transition at 560 nm. In addition superimposed transient absorptions are observed on both sides of the bleach. At 32 mJ/cm^2 photon flux, the bleaching is still visible at short delay times as a shallow local minimum in the broad absorption. It disappears almost completely within the first 100 ps, which is significantly faster compared to the low power bleach decay.
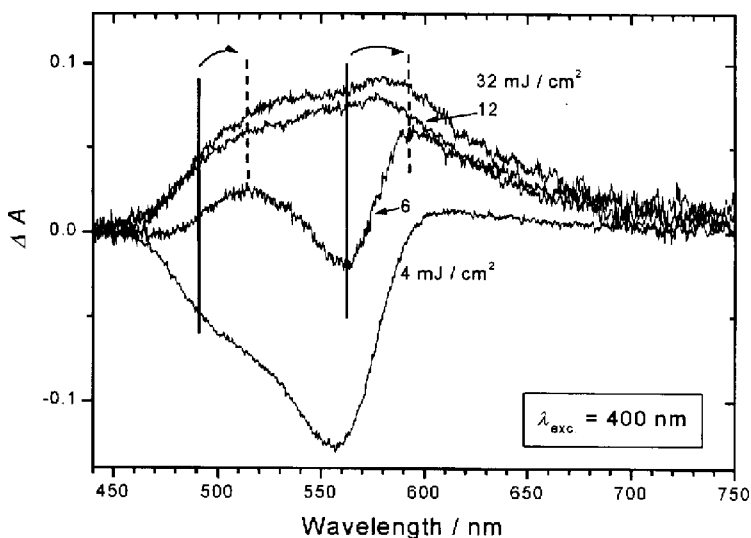

Fig. 2 Transient absorption spectra of CdSe NP pumped with different laser intensities of the second harmonics of an amplified Ti:Sapphire laser system yielding 100-fs pulses at 400 nm. The spectra with 6, 12, and 32 mJ/cm^2 are taken at 50 ps delay time between pump and probe pulse. The lowest power spectrum with 4 mJ/cm^2 is shown at a delay time of 2 ps to illustrate the original transitions at 480 and 560 nm. In the low pump power regime a transient bleach is observed. In the medium power regime both a bleach and red-shifted absorptions at 510 and 590 nm are found. With higher pump powers than 12 mJ/cm^{-2} the absorptions dominate the transient spectra. Moreover, a saturation effect can be observed, and the absorption does not change significantly for higher pump powers than 12 mJ/cm^{-2}.
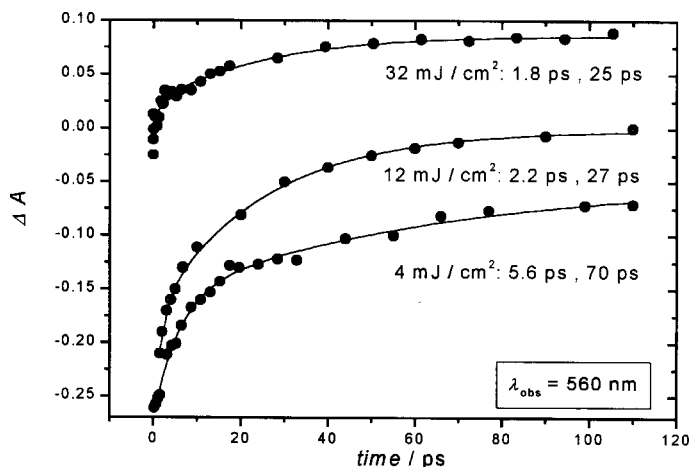
Fig. 3 The kinetic traces of the power-dependent bleach decay after excitation at 400 nm monitored at 560 nm, where the lowest exciton transition takes place. The bleach decay was found to be accelerated at increasing exciton densities, which was assigned to a higher trapping probability and possibly additional Auger processes (see text).

The changes in intensity and shape also indicate that at approximately 12 mJ/cm^2, a saturation of the high-density effect is reached. The spectral features of the 12- and 32-mJ/cm^2 spectra are not very different anymore. It was not possible to go higher in laser flux since the later experiments were carried out under highest available laser power and tightest beam focusing.

Figure 3 shows the corresponding kinetic traces of the bleach decay observed for three different pump intensities at the lowest exciton-transition (570 nm). For the decay of the bleach at the lowest pump power, two time components are resolved, one of 5.8 ps and one longer than 70 ps. The short-lifetime component of the transient suggests fast trapping by shallow traps. This is consistent with the observed shallow trap emission in our photoluminescence experiments 15. The slow component of the bleach decay (τ_2 in Fig. 1) is possibly due to trapping of the charge carriers by deeper traps [15]. For higher pump laser powers, the formation of the transient absorption is accelerated compared to the experiment with lower excitation intensity. This result is explained by the model, in which a higher density of excited charge carriers leads to a higher probability of trapping and/or a higher probability for Auger processes.

The spectrum in Fig. 2 at highest possible pump intensity shows a broad band from 460 to 700 nm. The question immediately arises as whether it is indeed a single band but gives the appearance of two bands at short delay times due to the intercepting bleach band. In order to answer this question, quenching experiments were carried out. As demonstrated in ref. 15 it is possible to transfer an excited conduction band electron of 4-nm-diameter CdSe NPs to an electron acceptor such as benzoquinone (BQ) adsorbed on the surface of the NP. We used this fact to see if this would change the band shape of the observed transient absorption in this region. Figure 4a shows that the addition of BQ leads to a quenching of the high-energy side of the absorption whereas the low-energy portion remains unchanged. This experiment supports unambiguously the assignment that the high pump-power-induced absorption consists of more than one band corresponding to different transitions. It is also found that the dynamics of the bleach decay are accelerated by the fast electron transfer to the adsorbed BQ, as demonstrated in Fig. 4b.

Nanoparticles with many surface traps: CdS NPs

For CdS NPs in aqueous solution it is relatively simple to prepare samples with well-defined modified surfaces. In order to understand the influence of the surface properties on the high-density absorption we prepared two CdS samples. The first sample was synthesized with a bare CdS surface without further
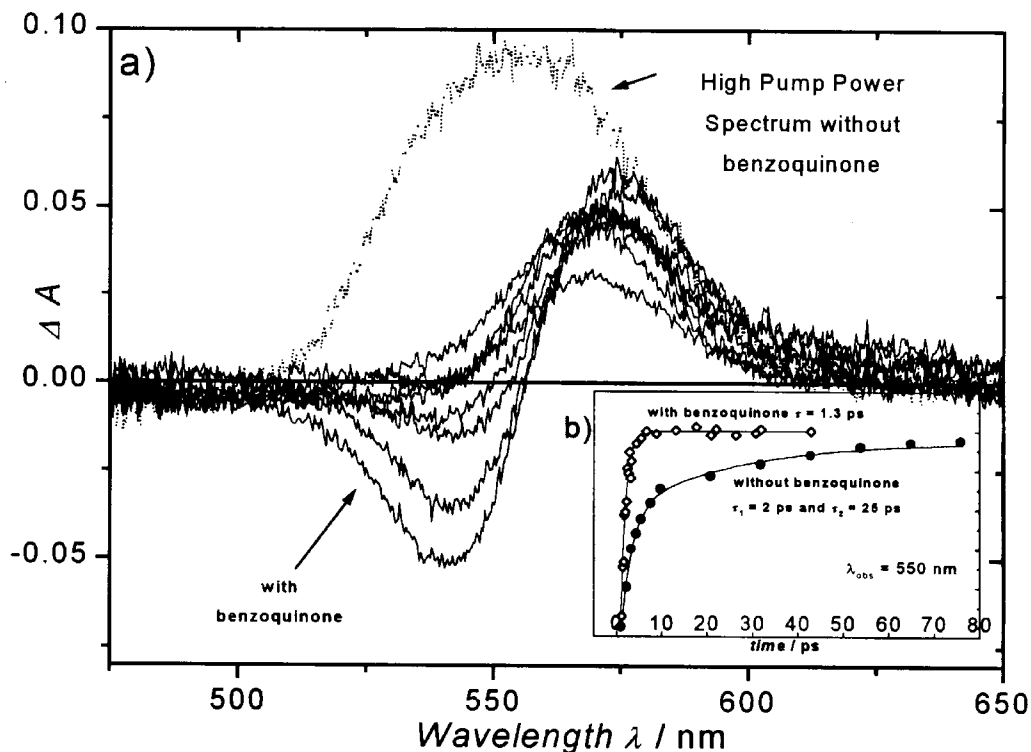
Fig. 4 a) Transient spectra of colloidal CdSe NPs excited with 32 mJ/cm^2 to achieve high exciton density. In the bare NP, without benzoquinone on the surface, the whole transient absorption feature is formed (dashed line). After addition of benzoquinone, the high-energy transitions are quenched showing that more than one transition contribute to the broad transient absorption band. The inset (b) shows the femtosecond dynamics of the quenched and unquenched system observed at 560 nm. The kinetic traces were normalized for better comparison of the different bleach decay kinetics. It is clearly visible that the addition of benzoquinone accelerates the bleach decay.

passivation steps. The second sample was passivated with CdOH [23]. From fluorescence quantum yield measurements [26,27], it is known that the near-band-edge emission quantum yield of NPs can be greatly enhanced by the addition of a OH$^-$ or a ZnS layer on the NP surface (passivation) [23]. In addition, after surface passivation the maximum of the luminescence is blue-shifted towards the band-edge energy. Therefore, it is concluded that this additional layer eliminates surface trapping sites [13]. Figure 5a shows the absorption and emission spectra of the two samples. It is clearly visible that the emission of the unpassivated sample shows a large portion of deep-trap emission, and the passivated one shows enhanced band-edge emission. If the high-density absorption spectra are due to trapped charge carriers on the NP surface, then a clear difference in the transient high-density spectra is expected. In Fig. 5b the high-power absorption of passivated and unpassivated CdS NPs of the same core size (4 nm diameter) are shown. It is found that the intensity of the transient absorptions of the unpassivated NPs are much higher. Also, the spectral position of the transient absorption did change, and a clear blue shift of the transient absorption was observed from the passivated to the unpassivated sample. The rise time of this absorption was faster than 200 fs, and its intensity did not change during the first 200 ps. The detailed analysis of the high-density spectroscopy on CdS NPs will be published elsewhere.
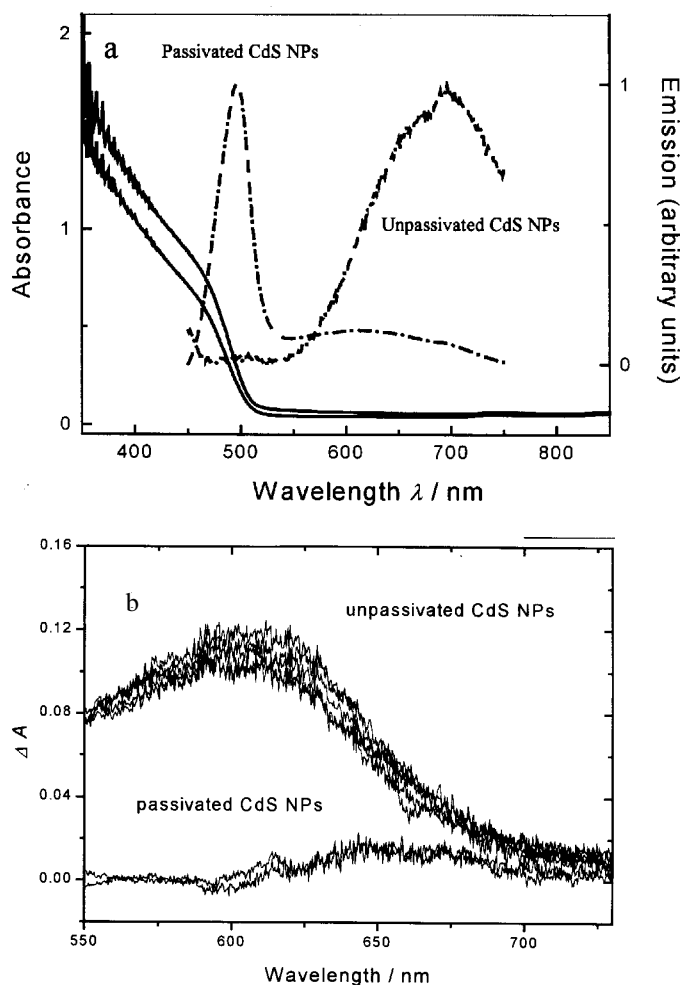
Fig. 5 a) The ground-state absorption and steady-state emission of two different CdS NP samples in water. The unpassivated sample shows strong deep-trap emission, which is almost completely—but not perfectly— quenched in the case of the surface-passivated sample. The passivated sample emits mainly at the band-edge energy and weakly at a wavelength between the band-edge- and deep-trap-emission wavelength. This indicates that surface passivation eliminates mainly the deep trapping sites. b) Femtosecond transient absorption spectra of CdS NPs 50 ps after laser excitation at 400 nm with 30 mJ/cm^2 to achieve high exciton density. The unpassivated CdS NPs show a much more intense absorption, which also takes place at higher energy than the absorption of the surface-passivated NPs. The decrease in transient absorption caused by the surface passivation suggests that the observed high-density absorption originates from surface-trapped charge carriers.

DISCUSSION

In the low-density regime, where only a single exciton is formed per NP, the observed phenomena can indeed be described by linear optics. Thus, the bleaching was explained with the band-filling of the charge carriers. With increasing excitation intensity, more excitons are formed per particle, and new high exciton density effects have to be taken into account. It is known [1,2] that the II-VI semiconductor

materials allow the simultaneous observation of several high-pump-power effects. From the spectroscopic point of view, it is an interesting challenge to identify the various contributions to the observed high-power-induced transient absorptions. It is suggested that they might result from one or more of the following mechanisms: 1) transient absorptions from a surface-trap state of the nanoparticle, 2) red-shifted exciton absorptions of the nanocrystal (corresponding to the bleach bands) induced by the internal Stark effect due to the high density of the free or trapped electrons and holes created by the multiple absorption in the particle itself, or 3) transitions to the bound bi- or multi-exciton (the complex formed from the electron-hole pairs) levels [1,28].

Absorption from a surface-trap state

The analysis of the bleach decay reveals an acceleration from 70 ps to 27 ps with increasing pump laser power. We therefore conclude that the observed new spectral shape and the accelerated bleach recovery is not due to a mixture of different excited NPs, but the sample is excited homogeneously. As only the intensity of the pump laser pulse is increased, the acceleration of the bleach recovery must be caused by the higher charge-carrier density. The apparent acceleration of the bleach recovery could then be explained either by a higher probability for the trapping of the excited charge carrier in the field of others or by a superposition of the bleach recovery and the kinetics for the new high-power-induced absorption feature. Additional Auger processes can not be excluded, but an increase in absorption on the red side (> 650 nm) of the transient spectra reminiscent for solvated electrons was not observed. It is possible, however, that the ejected charge carrier could be trapped on the particle surface and does not get completely ejected into the solvent. The high-power transient appears on an ultrashort time range (< 1 ps), whereas the bleach decays on the picosecond time scale.

Already Zhang et al. [18] proposed that the transient absorption at high power could be due to excitons or biexcitons in the conduction band when the shallow trap states are rapidly saturated [18]. In addition, power-dependent transient absorption observed in CdS, CdSe and CdZnS and Ag_2S NPs have been explained using this trap-state saturation model [19].

The transient high-power absorption spectra of the passivated and unpassivated CdS NPs in Fig. 5b reveal that the intensity of the transient absorptions of the surface-passivated NPs is much weaker. We conclude therefrom, that the transient absorption has to be assigned to charge carriers, which are trapped at the NP surface. Also, the spectral position of the transient absorption did change and a clear blue-shift of the transient absorption was observed for the unpassivated compared to the passivated sample. It seems that the passivation process eliminates mainly the deeper surface traps and not the shallow surface traps, since a low-energy transition is still observed. If these absorptions are indeed from surface-trap states of different depth, then the energy difference between the shallower (causing the 650-nm transition) and the deeper traps (the 600-nm transition) is 0.16 eV.

It needs to be pointed out that in NPs, even after trapping of the charge carriers at the surface (which is monitored by the bleach decay), the electron and hole are still bound by coulomb interactions, due to the spatial confinement. This induces a transient surface dipole moment (μ_S) in the particle. If the charge carriers are rapidly trapped at the surface, higher laser powers must lead to a higher density of trapped carriers. This holds up to a pump intensity where all the trapping sites are occupied by excited charge carriers. It was predicted by Hu et al. [29,30] that high (trapped) charge-carrier densities lead to additional transient absorptions due to exciton–biexciton transitions.

Trapped biexciton formation

The assignment of the transient absorption to trapped biexcitons might be supported by the fact that such absorptions have been observed for the bulk [32] in nanoparticles of 11 nm diameter in glass [20]
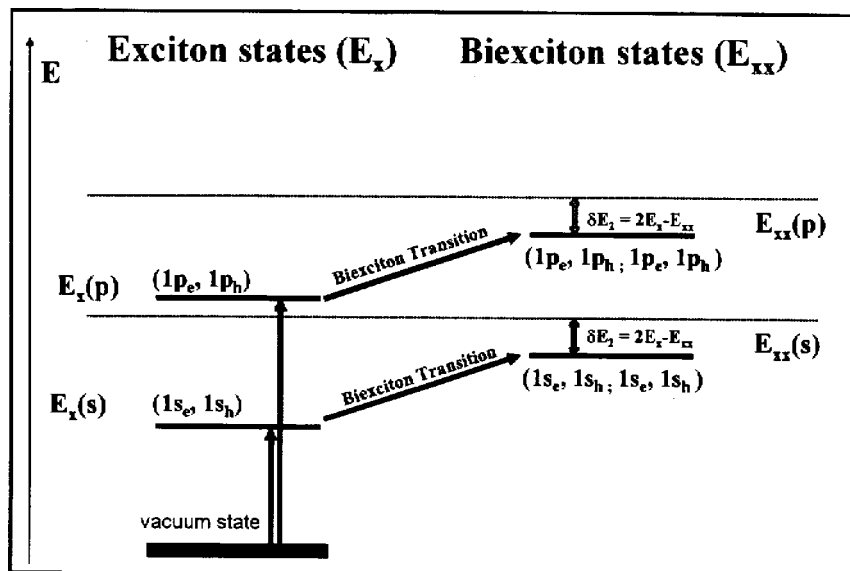
Fig. 6 A simplified picture for an internal Stark field effect due to filled surface traps. The energy of the Stark effect is drawn exaggerated for clarity. After trapping of the photoexcited charge carriers a surface field is established that lowers the energy of the internal electronic states. If the energy stabilization dominates over the band broadening, then this surface field leads to a red-shift of the exciton transition.

and has been predicted by theory by Park et al. [33] and Hvam et al. [32], who observed the direct two-photon absorption to a biexciton state in bulk CdSe by applying the differential transmission technique and determined a binding energy of 4.1 meV. They found that excitons bound to impurities enhance the two-photon absorption, as well as induce two-step transitions to the biexciton state. Their time-resolved measurements of the induced absorption revealed a lifetime of 600 ps of the bound exciton in bulk CdSe.

Due to the quantum confinement and its resulting enhancement of exchange and coulomb interaction the biexciton formation might be enhanced compared to the bulk material. Using numerical matrix diagonalization technique, Hu et al. have concluded that the biexciton stabilization energy of the order of the exciton binding energy [29,30] for particles of comparable size to those studied in the present work. They also observed experimentally photoinduced transient absorption at the low and the high energy sides of the bleach maximum [29] and simulated [30] their experimental results and assigned the induced transient absorptions to transitions between the exciton states and the biexciton ground and excited states.

If the observed transient absorptions are due to biexciton absorptions, the new absorption bands at 590 and 510 nm could be assigned to transitions to the biexciton ground state and its excited state levels (Fig. 6), as proposed by Klimov et al. [25]. The transition of interest is then the exciton–biexciton transition which should be observed in the same spectral range as the vacuum state–exciton transition. The biexciton binding energy is calculated from the equation $E_b = 2E_{exc} - E_{biexc}$ (twice the exciton energy minus the observed biexciton binding energy).

It is clear that the calculated value depends on which excitons form the observed biexciton with absorption at 590 nm. If the energy difference between the bleach minimum and the new absorption maximum is used for E_{exc}, the biexciton binding energy is calculated to be $E_b = 120 \pm 20$ meV. This is at least 20 times larger than that observed in the bulk (1.2–4.1 meV) [32] but in the order of that observed for the 11-nm particles in a glass (32 meV) [20]. This might be a manifestation of the more
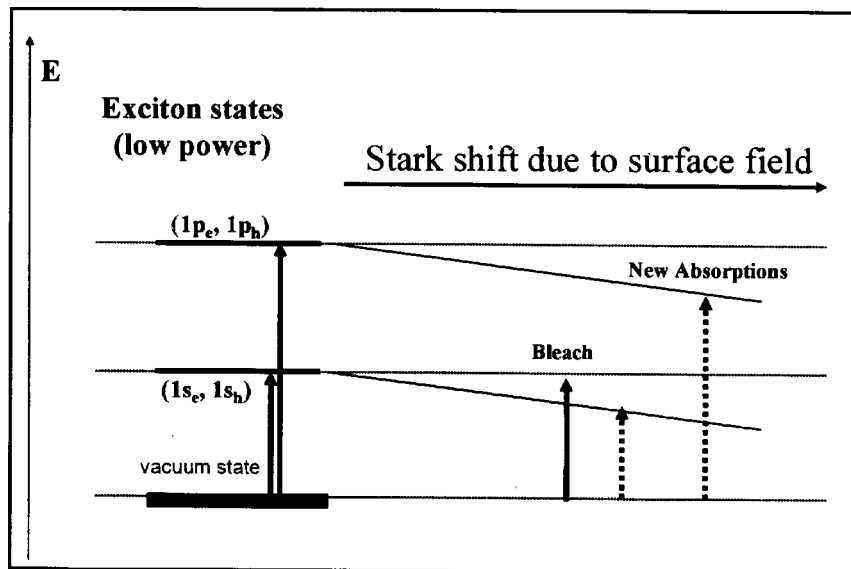
Fig. 7 The proposed picture for possible biexcitonic transitions from exciton (at the energy E_x) to biexciton states (E_{xx}). The biexciton transitions take place at the same energy than the exciton transition minus a biexciton stabilization energy δE_2. Again, the stabilization energy is exaggerated for clarity. The energy levels of trap states are not specifically distinguished in this picture.

severe quantum confinement of the biexciton in the 4-nm CdSe NPs. According to the theory by Hu et al. [29,30], the binding energy of the confined biexciton should increase with decreasing nanoparticle radius. It could be that the observed absorption assigned to the biexciton is due to the interaction of the two lowest energy "dark" excitons [34], then the binding energy is reduced by 30–40 meV to 70 meV.

Intraparticle Stark effect

Since at the excitation intensities in the high-power experiments more than 50 electron-hole pairs can be formed in the nanoparticle, it is possible that a Stark shift or broadening of the absorption could take place. Colvin et al. [31] published experiments in which a modulated external field of up to 64 kV/cm was used. From these studies, the dipole moment of the lowest energy exciton was estimated to be 32 D. A multiple excitation of an NP could lead to an even higher internal electric polarization leading to large internal Stark fields. If this interpretation is correct, the Stark-induced spectral changes should be sensitive to the level of the laser power and the delay time after excitation (i.e., sensitive to the number of electron-hole pairs in the nanocrystal), as schematically illustrated in Fig. 7. Thus, the transient absorption maxima in CdSe NPs should be more red-shifted when laser pulses of 32 mJ/cm^2 are used than when only 12-mJ/cm^2 pulses are applied. This is not observed and could be due to a too low spectral resolution and might suggest that the surface traps are saturated at relatively low pump intensities. This can also be concluded from the spectral saturation, which was demonstrated in Fig. 2. It seems that the number of surface-trapped charge-carriers in our CdSe NPs does not change significantly above the pump level of 12 mJ/cm^{-2}.

On grounds of the observations made we suggest the following contribution of internal Stark field to the formation of the transient absorptions. The shift results from the interaction between the free exciton dipole (32 D) and an internal field of a net surface dipole resulting from rapidly trapped surface excitons [31]. The net surface dipole does not vanish due to the asymmetry of the excitation with a

linear polarized laser field. Trapping might not completely randomize the initial nonisotropic excitation process. The particle being almost spherical, a good number of the dipoles would cancel one another due to the fact that while the initial dipole axes are parallel to the laser pump field, the signs of the induced dipoles could be positive or negative.

In a simplified approach [6], we use the electrostatic dipole approximation and the observed 120 meV shift ΔE to write down:

$$\Delta E = \frac{2\mu_s \mu_{Exc.}}{4\pi\varepsilon r^3} \tag{1}$$

where μ_S is the net surface dipole moment and $\mu_{Exc.}$ is that of the exciton [31] (32 D). If the distance between the two dipoles was set at r = 2 nm as an average value in our 4-nm nanoparticle and ε is $10 \times \varepsilon_o$ (ten times the vacuum permittivity) [31], one can calculate a maximum value of the average surface dipole moment μ_S = 24 D.

The model of an intrinsic electric field due to rapidly trapped charge carriers can also explain the weak sensitivity of the observed shift to the excitation power. As the pump power is increased, merely more particles are excited as the trapping sites in each particle saturate rapidly. Thus the intensity of the new absorptions increase up to a certain pump intensity, and from there on the interaction between the free and the net trap dipole in each particle remains constant. The lifetimes of the trapped charge carriers are very long (up to μs), thus explaining the persistence of the absorption on our time scale.

CONCLUSIONS

Even after careful preparation of the CdSe NPs used, the surface is not perfect and contains many trapping sites. We thus believe that trapping is an important relaxation process in nanoparticles. This is enhanced at high excitation densities as the rate of trapping increases. Thus, at large density the electrons and holes are expected to get rapidly localized at the various surface traps of the NPs. At least for small NPs, this surface-trap distribution is expected to be asymmetric, and the deviation from spherical symmetry results in a net intrinsic electric field. The transient absorption observed at high excitation densities (see Fig. 2), the intensity of these bands increases nonlinearly with pump power and reaches saturation at around 12 mJ/cm^2. Excitation with a higher photon flux did not increase the absorption. This is believed to be due to the saturation of the traps with the photoexcited charge carriers within individual nanoparticles.

As shown in Fig. 5, passivation of the NP surface seems to eliminate the transient absorptions except for a weak intensity at the red-tail end. The latter might reflect the thermodynamic or kinetic preference of the binding of the chemical used for passivation. The spectral changes are very similar to those observed after the addition of benzoquinone to the NP solution (Fig. 4). We believe that the quinone tends to be adsorbed on the most positively charged sites, which are also the deepest trapping sites. Therefore, the absorption at shorter wavelength is quenched whereas the one on the red-tail is not. In addition, it makes very good sense to argue that the lower trapping sites do not get occupied with excited charge carriers due to the interference of the surface electron acceptor.

The fact that we observe many surface traps also supports the other two proposed mechanisms. As the trap density increases, the density of surface-trapped bi- or higher excitons increases and it will lead to red-shifted absorption. In addition, the asymmetric distribution of the trapped electrons and holes could give rise to a net surface dipole that leads to the red-shift of the exciton energy. The high-density spectra are sensitive to the surface traps and thus allow us to probe the quality of the semiconductor NP surface.

ACKNOWLEDGMENTS

REFERENCES

1. S. V. Gaponenko. *Optical Properties of Semiconductor Nanocrystals,* Cambridge University Press, New York (1998).
2. C. F. Klingshirn. *Semiconductor Optics*, Springer, Berlin (1997).
3. P. Guyot-Sionnest, M. Shim, C. Matranga, M. Hines. *Phys. Rev. B*, **60**, 2181 (1999).
4. G. Cerullo, S. De Silvestri, U. Banin. *Phys. Rev. B*, **60**, 1928 (1999).
5. A. I. Ekimov, I. A. Kudryavtsev, M. G. Ivanov, Al. L. Efros. *J. Lum.*, **46**, 83 (1990).
6. C. Burda, T. Green, S. Link, M. A. El-Sayed. *J. Phys. Chem. B* **103***, 10775 (2000).
7. A. Haug. *J. Lumin.*, **20**, 173 (1979).
8. B. O'Reagan and M. Gratzel. *Nature*, **353**, 737 (1991); M. Nazeeruddin, A. Kay, I. Rodicio, R. Humphry-Baker, E. Muller, P. Liska, N. Vlachopoulos, M. Gratzel. *J. Am. Chem. Soc.* **115**, 6382 (1993). A. Kay and M. Gratzel. *J. Phys. Chem.*, **97**, 6272 (1993).
9. L. Brus, *Isr. J. Chem.* **33**, 9 (1993).
10. Y. Wang, A. Suna, J. McHugh, E. F. Hilinski, P. A. Lucas, R. D. Johnson. *J. Chem. Phys.* **92**, 6927 (1990).
11. V. Klimov, P. Haring Bolivar, H. Kurz. *Phys. Rev. B* **53**, 1463 (1996).
12. M. Nirmal, D. J. Norris, M. Kuno, M. G. Bawendi, Al. L. Efros, M. Rosen. *Phys. Rev. Lett.* **75**, 3728 (1995).
13. X. Ai, R. Jin, C. Ge, J. Wang, Y. Zou, X. Zhou, X. Xiao. *J. Phys. Chem.* **106**, 3387 (1997).
14. V. Klimov and D. McBranch. *Phys. Rev. B* **55**, 13173 (1997).
15. C. Burda, T. Green, S. Link, M. A. El-Sayed. *J. Phys. Chem. B* **103**, 1783 (1999).
16. R. B. Little, C. Burda, S. Link, S. Logunov, M. A. El-Sayed. *J. Phys. Chem. A* **102**, 6581 (1999).
17. S. Logunov, T. Green, S. Marguet, M. A. El-Sayed. *J. Phys. Chem. A* **102**, 5652 (1999).
18. M. C. Brelle, J. Z. Zhang, L. Nguyen, R. K. Mehrea. *Chem. Phys*, in press, special Kent Wilson issue (1999).
19. T. W. Roberti, N. J. Cherepy, J. Z. Zhang. *J. Chem. Phys.* **108**, 2143 (1998).
20. S. Hunsche, T. Dekorsy, V. Klimov, H. Kurz. *Appl. Phys. B* **62**, 3 (1996).
21. V. I. Klimov, Ch. J. Schwarz, D. W. McBranch, C. A. Leatherdale, M. G. Bawendi. *Phys. Rev. B*, **60**, 2177 (1999).
22. C. B. Murray, D. J. Norris, M. G. Bawendi. *J. Am. Chem. Soc.* **115**, 8706 (1993).
23. L. Spanhel, M. Haase, H. Weller, Henglein. A. *J. Am. Chem. Soc.* **109**, 5649 (1987).
24. S. Hunsche, T. Dekorsy, V. Klimov, H. Kurz. *Appl. Phys. B*, **62**, 3 (1996).
25. H. Klimov, S. Hunsche, H. Kurz. *Phys. Rev. B*, **50**, 8110 (1994).
26. M. L. Steigerwald and L. E. Brus. *Acc. Chem. Res.* **23**, 183 (1990).
27. H. Weller. *Adv. Mat.* **5**, 88 (1993).
28. U. Woggon. *Optical Properties of Semiconductor Quantum Dots,* Springer, New York (1996).
29. Y. Z. Hu, M. Lindberg, S. W. Koch. *Phys. Rev. B* **42**, 1713 (1990).

30. Y. Z. Hu, S. W. Koch, M. Lindberg, N. Peyghambarian, E. L. Pollock, F. Abraham. *Phys. Rev. Lett*. **64**, 1805 (1990).
31. V. L. Colvin and A. P. Alivisatos. *J. Chem. Phys.* **97**, 730 (1992).
32. K. H. Pantke, J. Erland, J. M. Hvam. *J. Cryst. Growth*, **117**, 763 (1992).
33. S. H. Park, R. A. Morgan, Y. Z. Hu, M. Lindberg, S. W. Koch, N. Peyghambarian. *J. Opt. Soc. Am. B* **7**, 2097 (1990).
34. M. Nirmal, D. J. Norris, M. Kuno, M. G. Bawendi, Al. L. Efros, M. Rosen. *Phys. Rev. Lett*. **75**, 3728 (1995).